

Single Pump-Valve Pneumatic Actuation With Continuous Flow Rate Control for Soft Robots

Sicong Liu¹, Member, IEEE, Lin Wang, Zhongfeng Qian, Dihan Liu, Wenpei Zhu¹, Shaowu Tang¹, Graduate Student Member, IEEE, Xuda Zhao, Wenjian Yang¹, Ying Lu, Juan Yi¹, Member, IEEE, Jian S. Dai¹, Fellow, IEEE, and Zheng Wang¹, Senior Member, IEEE

Abstract—Pneumatic actuated soft robots attract increasing interest of the researchers due to the availability and simplicity in actuation. The soft robots driven by soft pneumatic actuators (SPAs) of various active volumes demand pneumatic systems with various range of flow rate. However, the usually bulky and hard-to-carry pneumatic actuation systems restrict the portability, and the air pumps provide constant flow rate which constrained the applications such as soft wearable devices and scenarios require fine flow rate control. In this work, aiming for simplicity, high portability, continuous and small flow rate regulation, the pneumatic actuation system consists of identical integrated soft robotic drivers (iSoRD) modules is proposed, obtaining positive and negative pressure output ($-53\sim83$ kPa) in each module using one-pump-one-valve (4-way/2-position solenoid) design. With the check valves installed and the modular design, pressure holding and flow independence are achieved in each pneumatic branch. The heat generation (37.7°C) and power consumption (2.95 W per-channel) are measured to verify usability. The continuous and fine flow rate regulation (15 mL/s) is achieved by applying the PID controller on the pump motor, which shows superior performance in signal tracking in comparison with the non-continuous Bang-Bang and Varia-speed Bang-Bang algorithms. With the same control, the iSoRD system reduces the error by 37.5% in comparison to our previous two-pump system. The portability, versatility in wearing, practicality and adaptivity of the system are validated by driving

Received 2 August 2024; accepted 8 January 2025. Date of publication 17 January 2025; date of current version 29 January 2025. This article was recommended for publication by Associate Editor R. Diteesawat and Editor C. Laschi upon evaluation of the reviewers' comments. This work was supported in part by the NSFC under Grant 52475302, in part by the National Key R&D Program of China under Grant 2022YFB4701200, in part by Shenzhen Science and Technology Program under Grant JCYJ20220530114615034 and Grant JCYJ20220818100417038, and in part by the Guangdong Provincial Key Laboratory of Intelligent Morphing Mechanisms and Adaptive Robotics under Grant 2023B1212010005. (Sicong Liu, Lin Wang, and Zhongfeng Qian are co-first authors.) (Corresponding authors: Jian S. Dai; Zheng Wang.)

Sicong Liu is with the Sino-German College of Intelligent Manufacturing, Shenzhen Technology University, Pingshan 518118, China (e-mail: liusicong@sztu.edu.cn).

Lin Wang, Zhongfeng Qian, Juan Yi, and Zheng Wang are with Wisson Robotics, Shenzhen 518001, China (e-mail: wanglin@wissonrobotics.com; qianzf@wissonrobotics.com; yijuan2603@outlook.com; zheng.wang@ieee.org).

Dihan Liu, Wenpei Zhu, Shaowu Tang, Xuda Zhao, Wenjian Yang, Ying Lu, and Jian S. Dai are with the Department of Mechanical and Energy Engineering, Southern University of Science and Technology, Shenzhen 518000, China (e-mail: 11912532@mail.sustech.edu.cn; 11930368@mail.sustech.edu.cn; 12232306@mail.sustech.edu.cn; 12010325@mail.sustech.edu.cn; 12232351@mail.sustech.edu.cn; 11910835@mail.sustech.edu.cn; daijs@sustech.edu.cn).

This letter has supplementary downloadable material available at <https://doi.org/10.1109/LRA.2025.3531147>, provided by the authors.

Digital Object Identifier 10.1109/LRA.2025.3531147

three wearable soft robots, a small gripper and a pollination device. Comparing with the existing, the iSoRD is capable of fine flow rate regulation in both negative and positive pressure range with low power consumption, portability and versatility, which will benefit the pneumatic soft robotic systems with broadened application potential.

Index Terms—Soft robotic actuation, pneumatic actuation, continuous flow regulation.

I. INTRODUCTION

SOFT robotics emerges as one of the prosperous robotic fields, bringing enlightenment in aspects of robotic researches covering from design, fabrication to control. Benefiting from the properties of soft material, soft robots have dived into a wide range of application areas like deep-sea exploration [1], [2], [3], rehabilitation [4], [5], [6], robotic-assisted surgery [7], [8], [9], dexterous manipulation [10], [11], [12] and etc.

Pneumatic actuated soft robots attract interest of the researchers due to the availability and simplicity in actuation [13], [14]. Benefiting from the inherent compliance, soft robots driven by soft pneumatic actuators (SPAs) can interact with the external environment through safe and adaptive contacts [15], [16]. SPAs are much lighter than conventional actuators like electric motors and air pumps. Based on such merits, SPAs are suitable for constituting portable and wearable soft robotic systems which demand safe human-robot interaction, such as the exoskeletons that are lightweight and non-restrictive to the wearer [5], [6], [17], rehabilitation devices that provide convenient at-home use [4], [18], and supernumerary limbs [19], [20] that adaptively perform tasks interacting with objects of various rigidity and shape. While the typical functional end-effector such as the soft robotic glove are compliant and light weight in general, the restriction of the portability lies on the actuation systems, which are usually bulky and hard to be carried around due to the size, weight and complexity of the assembly. Also, the actuation system with constant air flow from the pump constrained the low-level control performance, which obstacles the soft devices to output smooth motions and the application on devices in need of small flow rate.

Pioneering research works were conducted on pneumatic actuation systems for soft robots, which can be categorized into two types according to the pressure generation mechanism: using syringe and using pump. Linear motor is used to push and pull syringe to regulate the pressure smoothly by continuous and high-bandwidth motion [21]. Sridar et al. [22] proposes

a portable pressure source in need of backpack-size space to accommodate the syringe and linear motor. Due to the compressibility of air, large cylinders and long-stroke linear motors are required to generate high pressure, which makes the system bulkier than solutions with pumps and valves. In contrast, the pump-valve system obtains portability, such as the fluid control board in [23] uses pumps as the pneumatic pressure source and solenoid valves to regulate the pressure. The pump-valve solution is shown to be effective and easy implementable for the soft robotic applications.

Much recent researches have achieved continuous flow rate regulation using dedicated valves in the pump and valve systems, such as the proportional valves in [20], [24] and the high-speed solenoid valves in [25]. But challenges remain, namely, the proportional valves request the minimum supply pressure higher than 200 kPa which is beyond the maximum pressure of the portable-sized pump at about 200 kPa, and using the high-speed switching of the solenoid valves (1000 Hz) to regulate the flow requires high power consumption about 40W. Thus, these solutions are yet to satisfy the requirements for simplicity and high portability. Recently, a novel actuation system is proposed in [26], which provides both positive and negative pressures using one pump and three solenoid valves to drive one actuator, regulates flow rate by two level of pump speed instead of using valve, showing the potential of using pump for flow rate control.

Pneumatic actuation systems cater to different gas volume or flow rate needs of a variety of applications, ranging from wearable robots [4], [5], [19], soft grippers, soft actuator, to pollen pollination with volume about 65 ml, 22 ml, 8 ml, and 0.33 ml, respectively, as illustrated in Fig. 1(a). To control airflow, micro-actuators often utilize a syringe pump or manual injection control [27]. Pollination devices for different flowers are required to apply varying amounts of pollen propell and regulate by the flow rate of the pneumatic source, and the conventional devices often rely on the large-scale spraying to ensure success-rate, which leads to wastage [28], [29], [30]. Therefore, a flow rate controllable pneumatic source with a extend range is needed for adaptivity and efficiency.

In this work, we propose a pneumatic actuation system with one pump and one valve in each channel providing continuous positive and negative pressures, with simple control logic and higher tracking accuracy to dynamic signals using continuous PID control. Such a system can be integrated into a flat and soft strip for versatile on-body wearing positions, driving soft robotic systems and a pollination device. The contribution of this paper can be summarized as follow:

- 1) A pneumatic actuation system consists of identical integrated soft robotic drivers (iSoRD) is proposed. With a simple one-pump-one-valve modular design, the iSoRD innovatively achieve fine flow rate regulation with low power consumption in both negative and positive pressure output when compared to the relevant actuation systems.
- 2) The continuous flow rate regulation is achieved by applying PID control on the pump of iSoRD, which achieves superior performance in pressure signal tracking when compared with the non-continuous control methods.
- 3) The iSoRD system show portability and adaptivity in demonstrations of driving a series of soft robotic devices and a pollination device. The excellence in delivering stable control over small flow rate is verified by experiments.

The paper is organized as follows. Section II proposes the pneumatic design, implementation and control of the iSoRD

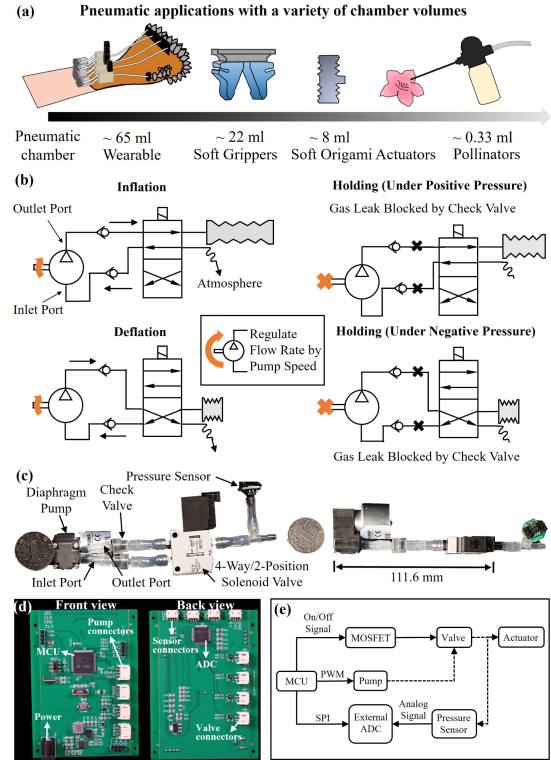


Fig. 1. Concept and design of the iSoRD pneumatic actuation. (a) The pneumatic system with identical integrated soft robotic drivers (iSoRD) is aimed to meet the requirement of soft robots and pneumatic devices with a range of chamber volumes and flow rates. (b) The structure, working modes and logic scheme of iSoRD. (c) The components and size measurement of an iSoRD unit. (d) The front view and back view of the control board integrated with microprocessors, connectors, etc. (e) The wiring and signal transmission logic on the control board.

system. Section III validates the performance and control of the pneumatic system in experiments. Section IV demonstrates the application on devices that demand different flow rates. A conclusion is drawn in Section V with future work presented.

II. DESIGN AND IMPLEMENTATION OF iSoRD

A. Pneumatic Design

An integrated unit that provides positive or negative pneumatic pressure for SPA and adjusts the rate of pressure change use only one small-sized pumps is in favor as shown in Fig. 1(b). While compact in dimensions, having the potential to realize pressure holding and flow rate control as the peristaltic pump in [42], the flow rate of diaphragm pump is about 5-6 times higher than that of the similar-sized peristaltic pump (about 200 ~ 300 ml/min), which provides sufficient performance to support the SPA for dynamic motions. Hence, diaphragm pump is chosen as the air source as shown in Fig. 1(c). Since the diaphragm pump use one-way valve to generate stable directional pneumatic flow, the flow direction of each port is fixed, i.e., the direction of flow cannot be regulated by changing the rotation direction of the motor in the pump. Thus, a 4-way/2-position (4W2P) solenoid valve is used to control the direction of flow.

As shown in the working logic of the pneumatic design in Fig. 1(b), when the actuator is connected to the outlet of the pump

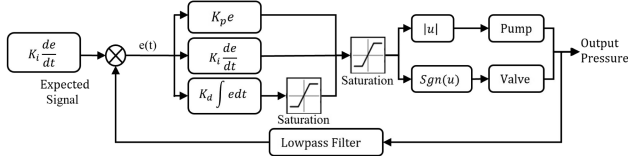


Fig. 2. The computing logic of the PID controller.

through the 4W2P valve and the inlet of the pump is connected to atmosphere, the actuator is in inflation state subjected to positive pressure. To change the direction of the flow, the actuator is switched to the inlet of the pump by the 4W2P valve and enter the deflation state under negative pressure. The flow rate is controlled by regulating the speed of the pump motor. To achieve pressure holding, two one-way check valves are installed between the pump and the 4W2P valve to prevent leakage. The check valve at the outlet port of pump prevents air to flow from the 4W2P valve back to the pump, and vice versa at the inlet port.

B. System Implementation

The implementation of an iSoRD unit is shown in Fig. 1(c), including a diaphragm pump (YW11-BLDC, Yuanwang Fluid Technology), a 4W2P solenoid valves (VQD1121-5L-M5, SMC), and a pneumatic pressure sensor (XGZP6857A, ±100 kPa, 1%, CFSensor Inc.). Both ports of the diaphragm pump are connected to the two 4W2P valves, and each branch has a one-way check valve to ensure airtightness. The resultant size of the iSoRD unit is measured 111.6 mm in length, 17.5 mm in width and 55.25 mm in height, with the profile approximately the size of the palm.

The integrated physical control hardware is shown in Fig. 1(d), with the wiring and signal transmission shown in Fig. 1(e). The optocoupler isolation module (BG0B-04N, Shenzhen Biaokong Co., Ltd.) is used to control the valve. The diaphragm pump is driven by a DC motor with a built-in driver board. The pump receives the control of Pulse-Width Modulation (PWM) signal from the MCU (STM32F767IGT6, STMicroelectronics) to regulate the motor speed continuously. The Analog-to-Digital Converter ADC (AD7606, Analog Devices, Inc.) transfers data with MCU through Serial Peripheral Interface (SPI). The size of the overall control board is 90 mm by 60 mm.

C. Control of iSoRD

The pump flow can be continuously adjusted by the motor, therefore, a continuous controller is needed to improve the accuracy and speed of the system. The complex and high dynamics of the pumps and valves, and the compressibility of air make it difficult to establish a stable control model for the iSoRD system, so a model-free control method is selected in this paper. The PID controller with saturation output was chosen due to its simplicity and efficiency. The block diagram of the controller is shown in Fig. 2. The PID controller takes the error between the target and feedback pressure as input. The PID controller formula is expressed as follows [31]:

$$u(t) = K_p e(t) + K_i \int e(t) dt + K_d \frac{de(t)}{dt}, \quad (1)$$

where $e(t) = P_{rT} - P_{rF}$ is the difference between the target pressure signal P_{rT} and the feedback signal P_{rF} . K_p , K_i and K_d are the proportional, integral, and derivative gains of the PID controller.

Due to the limitation of the pump speed, the integral term increases rapidly when tracking fast signals. When the error decreases, the residential integral value will keep the output of the system to be excessively large for a long period. Therefore, the integral of the error is processed as the saturation, which can be expressed as:

$$K_i \int_{t_0}^{t_s} e(\tau) d\tau = \begin{cases} I_{MAX}, & K_i \int_{t_0}^{t_s} e(\tau) d\tau > I_{MAX} \\ -I_{MAX}, & K_i \int_{t_0}^{t_s} e(\tau) d\tau < -I_{MAX} \end{cases}, \quad (2)$$

where I_{MAX} is the maximum allowed integral term. Since the output of PID controller is in the form of duty cycle, and the duty cycle value range is [0, 100], a saturation processing is added after the output of PID controller and is expressed as:

$$u(t) \begin{cases} 100, & u(t) > 100; \\ -100, & u(t) < -100. \end{cases} \quad (3)$$

The final output will be decomposed into two values, one value is the absolute value of the output, used to control the pump duty ratio, the other value is the symbol of the output to control the on/off of the valve.

III. EXPERIMENTAL VALIDATION

A. Airtightness and Flow Independence

To validate the pressure holding of iSoRD with check valves, two types of pneumatic circuits are configured with and without the check valves between the pump and 4W2P valve as shown in Fig. 3(a). Step signal is given as system input to switch the pressure of the actuator between positive and negative for the inflation and deflation, respectively. After reaching the given pressure, the system is controlled to stay in the holding stage. The airtight effect of the system is determined by observing the pressure change.

The experimental results are plotted in Fig. 3(b) and (c). In the deflation tests, the systems are given target pressure 80kPa, and in the inflation test 120 kPa. After reaching the target values, pressure in the system without the check valves start to change immediately after the system switched to the holding stage and eventually reached atmospheric pressure, indicating a constant leakage of air. In contrast, the pressures in the proposed system with check valves changes slightly at first. After a short period, the pressures reached to the constant values in both cases, validating the airtightness in the iSoRD.

The two-pump pneumatic actuation system developed in our previous works [32] is used to compare with the iSoRD as shown in Fig. 3(d). In the two-pump system, the positive and negative pressures are generated by the respectively assigned pumps, which provide pneumatic source for multiple channels. Each channel connects to an actuator through a valve. The pressure in each channel is regulated by the on and off of the valve. Since the total flows of the pumps are limited, when multiple actuators are driven simultaneous with the valves functioning, the flows in activated channels will interfere with each other due to pressure differences, causing unstable behaviors of the actuators. In contrast, each actuator is driven by an independent

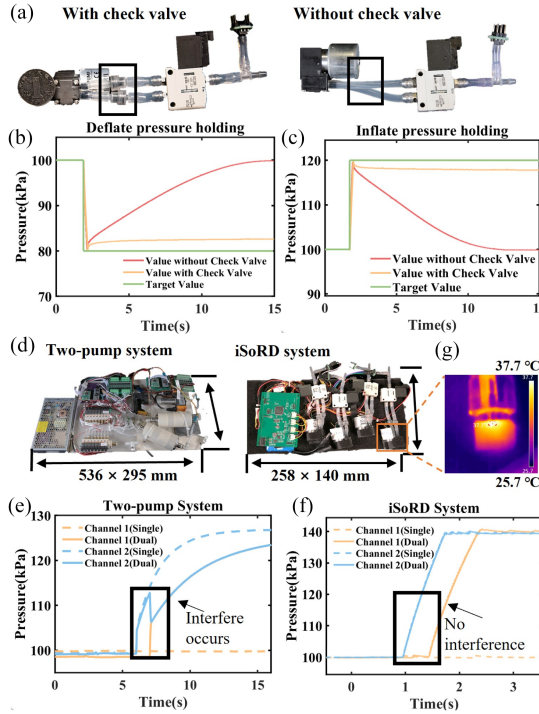


Fig. 3. Experimental validation on pressure holding and flow independence. (a) Experiment setup of the airtightness test. (b) Performance comparison of with and without check valve when holding negative pressure and (c) positive pressure. (d) Experiment setup of the flow independence performance on the two-pump system and the iSoRD system. (e) The sudden drops in the curves indicate the interference in the two-pump system. Single stands for only one channel are working in the system as the reference. Dual stands for both of the channels working simultaneously. (f) Flow independence performance of the iSoRDs system show no interference. (g) Thermal radiation of the pump.

unit in the proposed system, the flow paths of actuators are not connected which will avoid the interference.

The experiments are carried out in the iSoRD and two-pump systems with two channels connected with two bellows respectively. During the disturbance test, the two channels work simultaneously. In the two-pump system, two channels are connected when the valves are activated and the air pressure are neutralized to the same as shown in Fig. 3(e). Both of the curves show sudden drop behaviors, corresponding to the axial jitters of the actuators. While in the iSoRD system, there is no obvious change of the behavior in the actuators, indicating no interference in flow rate or pressure when two actuators are pressurized simultaneously as shown in Fig. 3(f). Thus, the iSoRD system drives the actuators without flow interference.

B. Power Consumption and Heat Generation

The power consumption of the iSoRD system is investigated in a free-load test, in which the pumps and valves are program to continuously run without load. The power consumption is recorded by the power supply instrument (UTi120S, Uni-Trend Co., Ltd.) as 11.8 W, and listed in Table I. Comparing with the existing systems, the proposed shows the lowest power consumption per-channel 2.95 W among the ones capable of the flow-rate regulation in both negative and positive pressure range.

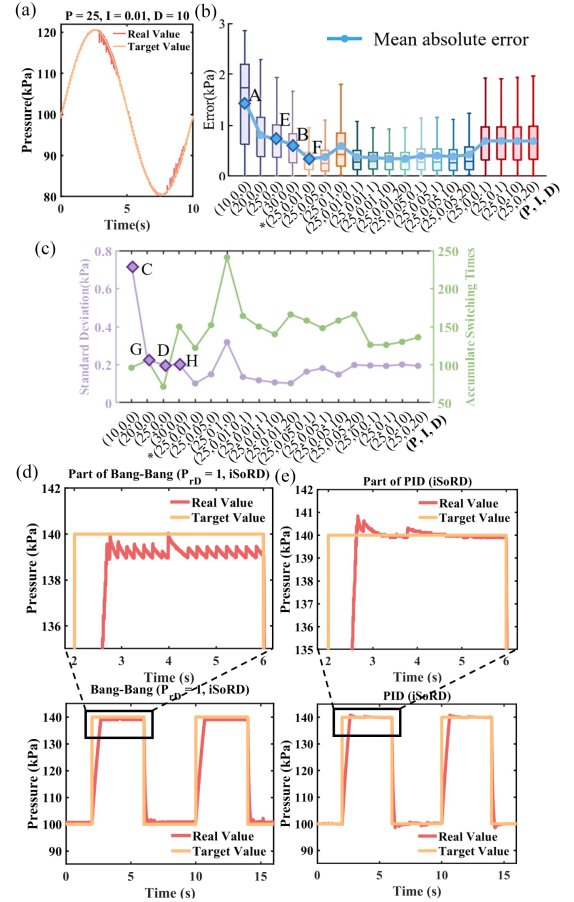


Fig. 4. Parameter tuning of PID controller and step signal tracking. (a) Performance of parameter set $P = 25$, $I = 0.01$, $D = 0$, as a typical example. (b) Absolute error distribution of tested parameter in PID parameter tuning, and the horizontal axis is the PID parameter sets. (c) Accumulated valve switching times and standard deviation of absolute error in PID parameter tuning, and the horizontal axis is the PID parameter sets. (d) Performance of non-continuous Bang-Bang control with dead zone of 1 kPa, and (e) PID control in step signal tracking are compared.

The heat generation of the iSoRD is measured in a test, where the pump was set to run full power for 10 mins. During the test, the maximum surface temperature is measured as 37.7 °Celsius (UTi120S, Uni-Trend Co., Ltd.) as shown in the recorded infrared image in Fig. 3(g). The heat generation is lower than that of the soft robotic wearable system's 41 °Celsius in [36] as listed in Table I, validating the acceptable heat generation and usability of iSoRD.

C. PID Continuous Control

To investigate the influence of the PID parameters on the performance of the iSoRD system (see Fig. 4(a)), three statistics are used: the mean absolute error (see Fig. 4(b)), which directly reflects the accuracy of controller, the standard deviation of absolute error and accumulated valve switching times (see Fig. 4(c)), which reflect the volatility of the control. The experiment is setup using a single iSoRD unit, Sine wave is chosen as the test signal with cycle time of $T = 10$ s and amplitude of 20 kPa.

PID parameters are regulated similar to the Ziegler-Nichols tuning method [33]. By regulating P term, the error reduces for

TABLE I
COMPARISON OF PNEUMATIC ACTUATION SYSTEMS FOR SOFT ROBOTICS

System Parameters	The single channel				The whole system			
	Pressure source	Solenoid valves	Flow rate (mL/s)	Relative pressure range (kPa)	Channels	Weight (g)	Size (mm)	Power consumption (W)
iSoRD [35]	1 Pump	1	15	-53~83	4	598.3	258 × 140 × 25	11.8
[36]	2 Pumps	2	216.7	0~310	2	3000	255 × 215 × 85	12
[37]	2 Pumps	2	8.3	-62.1~62.1	5	114	60 × 56 × 28	-
[4]	2 Pumps	1	28.3	-50~80	10	-	360 × 230 × 120	-
[26]	1 Pump	2	-	0~345	5	3300	-	19.5
[38]	1 Pump	3	20	-59~112	5	-	240 × 300 × 110	-
[39]	1 Pump	3	166.7	-	1	840	-	3
[40]	2 Pumps	2	66.7	0~150	5	1800	-	> 20
[41]	1 Pumps	3	-	0~100	5	283	-	1.12
	1 Pump	1	>15.3	0~300	2	7500	390 × 400 × 110	147

58% from point A ($P = 10$) to B ($P = 30$), the standard deviation reduces for 72% from point C ($P = 10$) to D ($P = 25$). Aim for fewer switching times of the motor direction, aside from low mean error and standard deviation, $P = 25$ is chosen. A small number of increments of the I term reduces mean error and standard deviation without increasing the switching times. The error is reduced for 50% from point E ($I = 0$) to F ($I = 0.01$), the standard deviation reduced for 48% from point G ($I = 0$) to H ($I = 0.01$). The D term brings limited benefit to system performance. Thus, the PI controller with $P = 25$ and $I = 0.01$ is suitable for the iSoRD system.

D. Comparison With Non-Continuous Control

To further validate the advantage of the PID continuous control in the iSoRD system against the non-continuous control, the Bang-Bang control and the Varia-speed Bang-Bang close loop control [34] are adopted and compared in the experiments. The Bang-Bang algorithm is described as,

$$\begin{cases} u = 100, & \text{when } P_{rF} > P_r + P_{rD}; \\ u = 0, & \text{when } P_r + P_{rD} > P_{rF} > P_r - P_{rD}; \\ u = -100, & \text{when } P_{rF} < P_r - P_{rD}, \end{cases}$$

where u is motor rotation rate, P_r is the pneumatic pressure, P_{rF} is the feedback pressure, P_{rD} is the pressure of dead-zone. And the Varia-speed close loop control is described as,

$$\begin{cases} u = 100, & \text{when } P_{rF} > P_r + P_{rD}, P'_{rF} > P'_r + P_{rD}; \\ u = 70, & \text{when } P_{rF} > P_r + P_{rD}, P_{rF} \leq P'_r + P_{rD}; \\ u = 0, & \text{when } P_r + P_{rD} > P_{rF} > P_r - P_{rD}; \\ u = -70, & \text{when } P_{rF} < P_r - P_{rD}, P_{rF} \geq P'_r + P_{rD}; \\ u = -100, & \text{when } P_{rF} < P_r - P_{rD}, P_{rF} < P'_r + P_{rD}, \end{cases}$$

where P'_r and P'_{rF} are the differentiation of P_r and P_{rF} , respectively.

The PID control and Bang-Bang with dead-zone pressure P_{rD} are tested on the iSoRD system to study the effect on the step signal tracking. We found in previous work [32] that lowering P_{rD} increases the oscillation of the soft robots' motions when controlled by Bang-Bang, due to the compressible nature of the gas and the compliance of the actuators and the structure. In addition, the pneumatic pressure sensor with accuracy of 1 kPa are used. Considering the sensor precision and oscillation

reduction, we set $P_{rD} = 1$ kPa, which result in a mean absolute error of 0.89 kPa as shown in Fig. 4(d). When applying PID control on the iSoRD system, the step response is smoothed with less visible oscillation as shown in Fig. 4(e). The mean absolute error is 0.32 kPa, which is a 64% drop compared to the Bang-Bang control.

The sinusoidal signals with different periods are tested to verify the effectiveness of the continuous control. The variation range of the period is 2–16 s. The amplitude of the signal is 20 kPa with median of 100 kPa. The experiment setup is shown as Fig. 5(a) with a single port of the iSoRD and the two-pump system connecting to a soft bellow actuator in each system. The influence on the mean error of the pressure and standard deviation are recorded and plotted in Fig. 5(b). The results show that the continuous control on the iSoRD system has better tracking effect and less fluctuation under all sinusoidal signals. With the same Bang-Bang control, the iSoRD system improve the performance, namely, there is a 37.5% drop in error in comparison to the two-pump system. When the period is shortened, the PID control performs stably with smaller error and standard derivation than Bang-Bang.

The performance of different control methods on the iSoRD system is further studied with $T = 10$ s. The result in Fig. 5(c) shows that Bang-Bang control can follow the trajectory, but with obvious oscillation around target pressure. The mean absolute deviation is about 0.81 kPa, and the standard deviation is 0.57 kPa. There is obvious static difference of tracking performance when Varia-speed Bang-Bang control is implemented, and the fluctuation value raises substantially as shown in Fig. 5(d), while the PID controller effectively constrains the fluctuation of pressure as shown in Fig. 4(a). When comparing with Bang-Bang control, the PID control obtains a 58.2% drop in error, a 44.1% drop in variance and a 78.6% drop in number of fluctuations. Comparing with Varia-speed Bang-Bang, PID controller reduces the error by 91.6%, and reduces the variance by 72.8%. The results are shown in Fig. 5(e) and (f).

E. Flow Rate Controllability

In order to measure the airflow output of the system, the experiment shown in Fig. 6(a) is established. The iSoRD system is connected to a pressure regulator and a syringe. By setting a push-rod into the syringe and adding weights on top of it, the airflow output of the system with loads can be measured, while

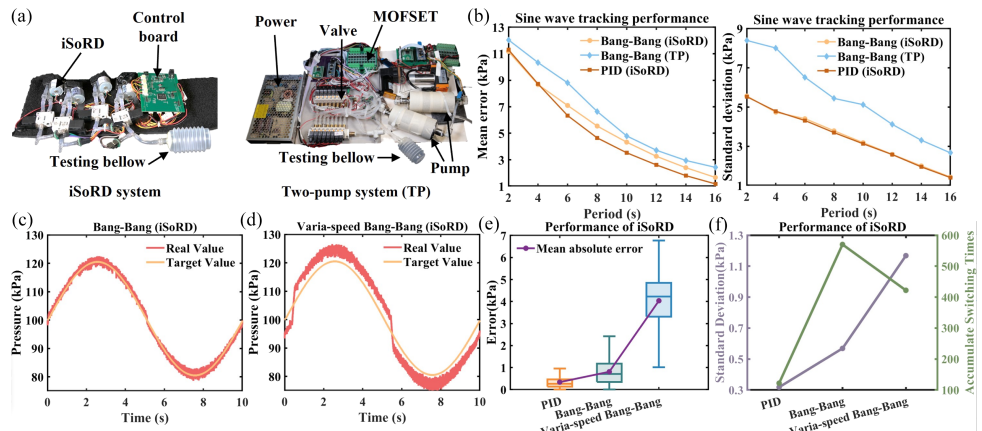


Fig. 5. Comparison with non-continuous control in Sine signal tracking. (a) Experiment setup. (b) Performance with different systems and controllers. (c) Performance of Bang-Bang control with iSoRD system. (d) Performance of Varia-speed Bang-Bang control with iSoRD system. (e) Absolute error distribution and (f) accumulated valve switching times and standard deviation of absolute error.

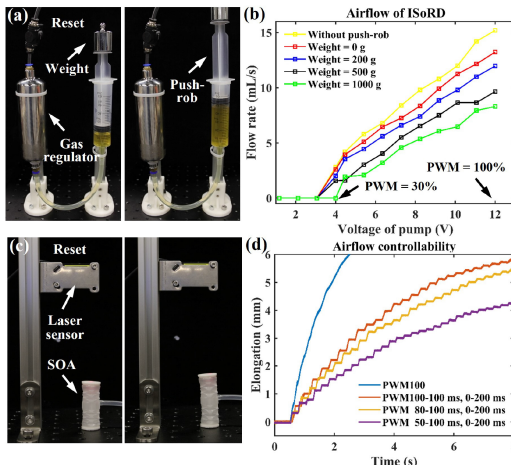


Fig. 6. (a) Experiment set up of airflow provided by the iSoRD system. (b) Output flow rate of the iSoRD system related to voltage of the pump and loads. (c) Experiment set up of airflow controllability. (d) Performance of airflow controllability. PWM 100-100 ms, 0-200 ms stands for the control mode which cycles between inflation with the duty cycle of 100% for 100 ms and the duty cycle of 0 (pause) for 200 ms.

the performance without the push-rod or load is recorded as comparison. Fig. 6(b) shows the relationship between flow rate and pump voltage. The operational voltage range of the pump, from 0 to 12 V, linearly corresponds to the PWM duty cycle, ranging from 0 to 100%. Without a proportional valve, the pump in the iSoRD system can operate at a minimum duty cycle of 30%, resulting in a small airflow of 2.8 ml/s. When the pump operates at 100% duty cycle, it achieves the maximum airflow of 15 ml/s.

As shown in Fig. 6(c), the iSoRD system is connected to the lightweight small soft origami actuator (SOA, 8 ml) [19] to validate the controllability of the output airflow. The iSoRD system operates in the open-loop control modes, cycling between duty cycles of 100% (inflation) and 0% (pause). 4 control modes regulate the elongation speed of the SOA and the displacement is measured by a laser sensor, as shown in Fig. 6(d). The SOA elongates continuously with a 100% duty cycle, while in other

modes, the elongation of the SOA exhibits a stepwise trend with a consistent step height respective to the inflation flow rate. This indicates that the iSoRD system produces a stable and controllable air volume by the use of the motor duty cycles.

The state-of-the-art pneumatic actuation systems for soft robotics are compared in Table I, where the iSoRD system is able to continuously regulate the flow using the pump motor without additional components, consists of only one pump and one solenoid valve in each pneumatic branch, provides positive and negative pressure states, continuous flow rate regulation and stable output of low flow rate.

IV. APPLICATIONS ON PNEUMATIC DEVICES

A. Soft Wearable Devices

In order to achieve the portability and enable versatile wearing on human body, the components of the pneumatic system need to be flexibly arranged to form a flat and narrow profile conforming to human body. Thus, the prototype of the system is designed in the form of a soft strap. Since the dimensions of body parts vary, such as arm, wrist, shank, thigh, and etc., the positions of components need to be adjustable to cater to different operating conditions. The hook and loop fasteners were used to fix the components for the easy assembly and adjustability as shown in Fig. 7(a). An elastic strap with hook surface is used to wrap around the upper surfaces of the components to restrict movements and ensure stability. In this way, it is easy for the user to wear and fasten the actuation strap on the desired part of the body as shown in Fig. 7(b), (c) and (d).

The iSoRD system of 4 independent modules is then used to drive a series of soft devices to verify practicality, including the rehabilitation glove, supernumerary limbs [19] and rehabilitation wrist brace [5] as shown in Fig. 7(e)–(h). The devices are worn on the user and driven by the iSoRD system to move according to the predetermined functions. The rehabilitation glove straightens the index finger to 179° and bends to 148° within 10 seconds as shown in Fig. 7(e), and this finger is actuated by only a single iSoRD. The wrist rehabilitation brace (actuated by two iSoRDs) turns the wrist left and right and reaches about 20° within 7.5 seconds in each direction as shown in Fig. 7(f). The

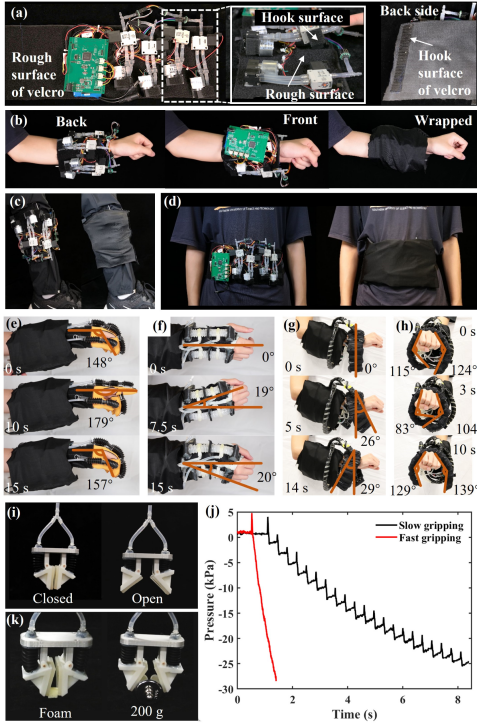


Fig. 7. iSoRD system application on soft robotic wearable devices and gripper. (a) The design that is soft, flat and adjustable, which can be worn on (b) wrist, (c) shank and (d) waist. (e) The rehabilitation gloves. (f) The wrist rehabilitation embrace. (g) The side view and (h) front view of supernumerary limbs. (i) A small gripper is driven by the iSoRD. (j) The slow and fast gripping are compared with the flow rate control of iSoRD. (k) The gripper can grasp a foam cube under slow gripping mode and successfully grip a weight of 200 g under both modes.

supernumerary limbs move in two directions and are actuated by two iSoRDs. The limb bends forward 26° and back 29° within 14 seconds on the side view as shown in Fig. 7(g). On the front view the left limb bends to 83° and straightens to 129°, and the right limb wraps outside of the left limb to 104° and straightens to 139° within 10 seconds as shown in Fig. 7(h). These devices perform the desired movements under the actuation of iSoRD system, proving the practicality in driving soft robotic wearable devices.

B. Small-Scale Pneumatic Gripper

An iSoRD module is further used to actuate the small-scale pneumatic gripper with the chamber volume of 22 ml (11 ml each actuator) as shown in Fig. 7(i)–(k). The system operates in two modes: fast gripping and slow gripping. Fast gripping employs open-loop control with a duty cycle of 100% of the motor. Slow gripping adopts a control which cycles between a 50 ms inflation with a duty cycle of 100% and a 300 ms pause with a duty cycle of 0. The opening and closing of the small-scale pneumatic gripper are shown in Fig. 7(i). In fast gripping mode (see Fig. 7(j)), the small-scale gripper completes the opening action within 2 seconds when the iSoRD system provides a high flow rate. In slow gripping mode, the pressure in the small gripper exhibits a stepwise pattern, resulting in minimal motion feed, making it suitable for grasping fragile objects. As shown in Fig. 7(k), the gripper can grasp a foam cube under slow gripping mode when the deformation of the foam is minimal. Under both gripping modes, the small-scale gripper can successfully grip a weight

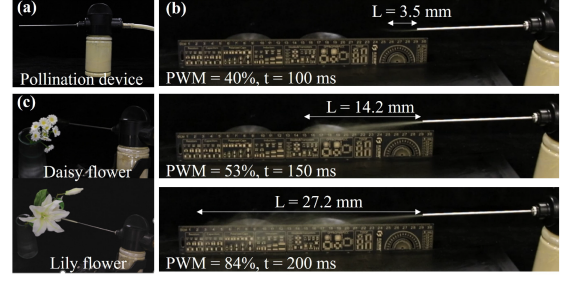


Fig. 8. iSoRD system actuates (a) the artificial pollination device. (b) The distance and quantity of ejected pollen are controlled by the iSoRD. (c) The pollination experiment on flowers of different sizes.

of 200 g. The tests demonstrate the iSoRD system is capable of providing fine control for minute movements and delivering sufficient force when required.

C. Flower Pollination

An artificial pollination device with the needle volume of 0.33 ml (diameter 1.85 mm, length 121 mm), is loaded with pollen and connected with one iSoRD module is shown in Fig. 8(a). The ejection distance of the pollen is measured with a ruler and recorded by videos. The ejection distance and quantity of the pollen are controlled by adjusting the duty cycle of the motor and ejection time t . With duty cycles of 40%, 53%, and 84%, the maximum ejection distances are 3.5 mm, 14.2 mm, and 27.2 mm, respectively, as shown in Fig. 8(b). The pollination experiments are further conducted on the artificial flowers of different sizes as shown in Fig. 8(c), where the ejected pollens successfully cover the pistils with concentrated and purposeful pollination effect, showing the application potential of the iSoRD system for scenarios in need of delicate control of airflow.

V. CONCLUSION

The iSoRD pneumatic actuation system consists of identical modules proposed, obtaining flow rate control in positive and negative pressure output ($-53\text{--}83$ kPa) in each module using one-pump-one-valve (4-way/2-position solenoid) design and PID control. With the check valves installed, pressure holding and flow independence are achieved in each pneumatic branch. With flow rate capability (2.8~15 ml/s), heat generation (37.7°C) and power consumption (2.95 W per-channel) investigated by experiments, the usability is verified.

The continuous flow rate regulation is achieved using the PID controller on the pump motor of the iSoRD. When compared to the non-continuous Bang-Bang control, the PID controller obtains 64% drop in mean absolute error in the step signal tracking; constrains the fluctuation of pressure with 58.2% drop in error, 44.1% drop in variance and 78.6% drop in number of fluctuations in the Sine signal tracking. Comparing with the non-continuous Varia-speed Bang-Bang, the controller reduces the error by 91.6%, and reduces the variance by 72.8%.

When tracking the Sine signal with the same Bang-Bang control, the iSoRD reduces the error by 37.5% in comparison to the two-pump system, proving the advantage of the simple pneumatic design. Comparing with the state-of-the-art pneumatic actuation systems for soft robots, the simple-structured modular system is capable of fine flow rate regulation in both negative and positive pressure range with low power consumption.

The portability and versatility of the system are shown in the 4-module system that is integrated into a flat and low-profile adjustable soft strip. The practicality of the system is validated by driving three soft wearable robots to output desired movements. The applications of driving a small-scale pneumatic gripper and a pollination device show the adaptivity of this system due to the range, the continuous and fine control of flow rate. The simplicity, portability, versatility, practicality and the continuous regulation of flow of the iSoRD system will benefit the pneumatic soft robotic systems with wider application potential. Future work includes further investigations on the accuracy, controllable range and applications of this system.

REFERENCES

- [1] G. Li et al., "Self-powered soft robot in the Mariana Trench," *Nature*, vol. 591, no. 7848, pp. 66–71, 2021.
- [2] K. C. Galloway et al., "Soft robotic grippers for biological sampling on deep reefs," *Soft Robot.*, vol. 3, no. 1, pp. 23–33, 2016.
- [3] Z. Shen et al., "Soft origami optical-sensing actuator for underwater manipulation," *Front. Robot. AI*, vol. 7, 2021, Art. no. 616128.
- [4] P. Polygerinos, Z. Wang, K. C. Galloway, R. J. Wood, and C. J. Walsh, "Soft robotic glove for combined assistance and at-home rehabilitation," *Robot. Auton. Syst.*, vol. 73, pp. 135–143, 2015.
- [5] S. Liu et al., "A compact soft robotic wrist brace with origami actuators," *Front. Robot. AI*, vol. 8, 2021, Art. no. 614623.
- [6] T. Proietti et al., "Sensing and control of a multi-joint soft wearable robot for upper-limb assistance and rehabilitation," *IEEE Robot. Automat. Lett.*, vol. 6, no. 2, pp. 2381–2388, Apr. 2021.
- [7] Z. Wang, S. Liu, J. Peng, and M. Z. Chen, "The next-generation surgical robots," *Surg. Robot.*, pp. 3–20, Jan. 2018.
- [8] G. Fang et al., "Soft robotic manipulator for intraoperative MRI-guided transoral laser microsurgery," *Sci. Robot.*, vol. 6, no. 57, 2021, Art. no. eabg5575.
- [9] J. Lai, K. Huang, B. Lu, Q. Zhao, and H. K. Chu, "Verticalized-tip trajectory tracking of a 3D-printable soft continuum robot: Enabling surgical blood suction automation," *IEEE/ASME Trans. Mechatron.*, vol. 27, no. 3, pp. 1545–1556, Jun. 2022.
- [10] S. Abondance, C. B. Teeple, and R. J. Wood, "A dexterous soft robotic hand for delicate in-hand manipulation," *IEEE Robot. Automat. Lett.*, vol. 5, no. 4, pp. 5502–5509, Oct. 2020.
- [11] W. Zhu et al., "A soft-rigid hybrid gripper with lateral compliance and dexterous in-hand manipulation," *IEEE/ASME Trans. Mechatron.*, vol. 28, no. 1, pp. 104–115, Feb. 2023.
- [12] J. Zhou, J. Yi, X. Chen, Z. Liu, and Z. Wang, "BCL-13: A 13-DOF soft robotic hand for dexterous grasping and in-hand manipulation," *IEEE Robot. Automat. Lett.*, vol. 3, no. 4, pp. 3379–3386, Oct. 2018.
- [13] R. Kang, Y. Guo, L. Chen, D. T. Branson, and J. S. Dai, "Design of a pneumatic muscle based continuum robot with embedded tendons," *IEEE/ASME Trans. Mechatron.*, vol. 22, no. 2, pp. 751–761, Apr. 2017.
- [14] J. Shintake, V. Cacucciolo, D. Floreano, and H. Shea, "Soft robotic grippers," *Adv. Mater.*, vol. 30, no. 29, 2018, Art. no. 1707035.
- [15] S. Yang et al., "Dynamic capture using a traplike soft gripper with stiffness anisotropy," *IEEE/ASME Trans. Mechatron.*, vol. 28, no. 3, pp. 1337–1346, Jun. 2023.
- [16] A. Ghafoor, J. S. Dai, and J. Duffy, "Stiffness modeling of the soft-finger contact in robotic grasping," *J. Mech. Des.*, vol. 126, no. 4, pp. 646–656, 2004.
- [17] Y. M. Zhou, C. Hohimer, T. Proietti, C. T. O'Neill, and C. J. Walsh, "Kinematics-based control of an inflatable soft wearable robot for assisting the shoulder of industrial workers," *IEEE Robot. Automat. Lett.*, vol. 6, no. 2, pp. 2155–2162, Apr. 2021.
- [18] P. Polygerinos et al., "Towards a soft pneumatic glove for hand rehabilitation," in *Proc. IEEE/RSJ Int. Conf. Intell. Robots Syst.*, 2013, pp. 1512–1517.
- [19] S. Liu et al., "Otariidae-inspired soft-robotic supernumerary flippers by fabric kirigami and origami," *IEEE/ASME Trans. Mechatron.*, vol. 26, no. 5, pp. 2747–2757, Oct. 2021.
- [20] P. H. Nguyen, C. Sparks, S. G. Nuthi, N. M. Vale, and P. Polygerinos, "Soft poly-limbs: Toward a new paradigm of mobile manipulation for daily living tasks," *Soft Robot.*, vol. 6, no. 1, pp. 38–53, 2019.
- [21] A. D. Marchese, K. Komorowski, C. D. Onal, and D. Rus, "Design and control of a soft and continuously deformable 2D robotic manipulation system," in *Proc. IEEE Int. Conf. Robot. Automat.*, 2014, pp. 2189–2196.
- [22] S. Sridar, S. Poddar, Y. Tong, P. Polygerinos, and W. Zhang, "Towards untethered soft pneumatic exosuits using low-volume inflatable actuator composites and a portable pneumatic source," *IEEE Robot. Automat. Lett.*, vol. 5, no. 3, pp. 4062–4069, Jul. 2020.
- [23] D. P. Holland et al., "The soft robotics toolkit: Strategies for overcoming obstacles to the wide dissemination of soft-robotic hardware," *IEEE Robot. Automat. Mag.*, vol. 24, no. 1, pp. 57–64, Mar. 2017.
- [24] P. Abbasi, M. A. Nekoui, M. Zareinejad, P. Abbasi, and Z. Azhang, "Position and force control of a soft pneumatic actuator," *Soft Robot.*, vol. 7, no. 5, pp. 550–563, 2020.
- [25] M. Hofer and R. D'Andrea, "Design, modeling and control of a soft robotic arm," in *Proc. IEEE/RSJ Int. Conf. Intell. Robots Syst.*, 2018, pp. 1456–1463.
- [26] B. Zhang, J. Chen, X. Ma, Y. Wu, X. Zhang, and H. Liao, "Pneumatic system capable of supplying programmable pressure states for soft robots," *Soft Robot.*, vol. 9, no. 5, pp. 1001–1013, 2022.
- [27] S. Konishi and H. Kosawa, "High-output bending motion of a soft inflatable microactuator with an actuation conversion mechanism," *Sci. Reports*, vol. 10, no. 1, 2020, Art. no. 12038.
- [28] M. A. Aizen and L. D. Harder, "Expanding the limits of the pollen-limitation concept: Effects of pollen quantity and quality," *Ecology*, vol. 88, no. 2, pp. 271–281, Feb. 2007.
- [29] K. Li, Y. Huo, Y. Liu, Y. Shi, Z. He, and Y. Cui, "Design of a lightweight robotic arm for Kiwifruit pollination," *Comput. Electron. Agriculture*, vol. 198, 2022, Art. no. 107114.
- [30] P. Pandey, J. J. Acosta, K. G. Payn, and S. N. Young, "Towards aerial robotic pollination for controlled crosses in *Pinus taeda*," in *Proc. ASABE Annu. Int. Meeting*, 2022, pp. 1–9.
- [31] R. C. Panda, *Introduction to PID Controllers: Theory, Tuning and Application to Frontier Areas*. Rijeka, Croatia: InTech, 2012.
- [32] Z. Fang et al., "Omnidirectional compliance on cross-linked actuator coordination enables simultaneous multi-functions of soft modular robots," *Sci. Reports*, vol. 13, 2023, Art. no. 12116.
- [33] V. V. Patel, "Ziegler-Nichols tuning method," *Resonance*, vol. 25, no. 10, pp. 1385–1397, 2020, doi: [10.1007/s12045-020-1058-z](https://doi.org/10.1007/s12045-020-1058-z).
- [34] C. Della Santina, C. Duriez, and D. Rus, "Model-based control of soft robots: A survey of the state of the art and open challenges," *IEEE Control Syst. Mag.*, vol. 43, no. 3, pp. 30–65, Jun. 2023.
- [35] T. Proietti et al., "Restoring arm function with a soft robotic wearable for individuals with amyotrophic lateral sclerosis," *Sci. Transl. Med.*, vol. 15, no. 681, 2023, Art. no. eadd1504.
- [36] A. Shtarkanov, "FlowIO development platform—The pneumatic 'Raspberry Pi' for soft robotics," in *Proc. Extended Abstr. CHI Conf. Hum. Factors Comput. Syst.*, 2021, pp. 1–6.
- [37] Y. Tian, R. Su, X. Wang, N. B. Altin, G. Fang, and C. C. L. Wang, "OpenPneu: Compact platform for pneumatic actuation with multi-channels," in *Proc. IEEE/ASME Int. Conf. Adv. Intell. Mechatron.*, 2023, pp. 765–770.
- [38] M. Ahlquist, R. Jitosho, J. Bao, and A. M. Okamura, "phloSAR: A portable, high-flow pressure supply and regulator enabling untethered operation of large pneumatic soft robots," in *Proc. IEEE 7th Int. Conf. Soft Robot.*, 2024, pp. 28–33.
- [39] J. Lai et al., "A novel soft glove utilizing honeycomb pneumatic actuators (HPAs) for assisting activities of daily living," *IEEE Trans. Neural Syst. Rehabil. Eng.*, vol. 31, pp. 3223–3233, 2023.
- [40] J. Qi et al., "HaptGlove—Untethered pneumatic glove for multimode haptic feedback in reality–virtuality continuum," *Adv. Sci.*, vol. 10, no. 25, 2023, Art. no. 301044.
- [41] B. P. Banyarani, T. Bahram, and H. Alireza, "Design and fabrication of a soft wearable robot using a novel pleated fabric pneumatic artificial muscle (pfPAM) to assist walking," *Sensors Actuators A, Phys.*, vol. 370, 2024, Art. no. 115278.
- [42] S. Wu et al., "High-performance hydraulic soft robotic control using continuous flow regulation and partial feedback," *IEEE Robot. Automat. Lett.*, vol. 9, no. 8, pp. 6967–6974, Aug. 2024.